School of Life Science and Technology, China Pharmaceutical University, Nanjing, P.R. China

A cell-internalizing peptide endows tumstatin7 with enhanced antitumor properties

Fanwen Wang, Ran Zhang, Bin Li, Qingqing Li, Heng Zheng, Xingzhen Lao*

Received July 1, 2018, accepted August 6, 2018

**Corresponding author: Xingzhen Lao, School of Life Science and Technology, China Pharmaceutical University, Nanjing, 210009, P.R. China*
lao@cpu.edu.cn

Pharmazie 73: 715–720 (2018) *doi: 10.1691/ph.2018.8623*

Tumstatin7 (CNYYSNS) is an antitumor peptide derived from the NC1 domain of Type IV collagen that has been associated with tumor angiogenesis. In this work, we generated a peptide composed of tumstatin7 fused to TAT, a cell-internalizing peptide consisting of 11 amino acids. Tumstatin7-TAT was internalized by cells and triggered cell death. The new peptide was more potent in inducing B16F10 melanoma cell apoptosis *in vitro* than the shorter tumstatin7. Whereas tumstatin7-TAT significantly reduced tumor cell viability, tumstatin7 showed only weak effects even at the highest treatment concentration applied. Both tumstatin7-TAT and tumstatin7 inhibited cell migration in an *in vitro* wound healing model, and the former was more effective than the latter in inhibiting tumor growth *in vivo*. Combining the cell-internalizing property of TAT with the tumor-specific property of tumstatin7 may provide a useful adjunct to tumor therapy.

1. Introduction

Tumstatin, a cleavage fragment from the collagen alpha 3 (IV) NC1 domain, possesses anti-angiogenic and anti-tumor cell activities; these two anti-tumor properties may be regulated by RGD-independent integrin beta3-mediated mechanisms (Maeshima et al. 2000a,b, 2002; Sudhakar et al. 2003). A clear and inverse correlation between tumor vascularization and tumstatin expression has been observed in bronchopulmonary human carcinomas (Caudroy et al. 2004; Pasco et al. 2004).

Previous studies have shown that the NC1a3(IV)-(185–203) peptide of tumstatin is responsible for binding with alpha v beta 3 (αvβ3) integrin in a vitronectin/fibronectin /RGD cyclic peptide-independent manner, leading to "outside-in" transduction signaling (Fawzi et al. 2000; Shahan et al. 1999; Sudhakar et al. 2003). The NC1a3(IV)-(185–203) peptide also displays specific anti-tumor properties by inhibiting the proliferation and invasion abilities of melanoma and other various cancer cells (Han et al. 1997; Pasco et al. 2000a,b).

A YSNSG cyclopeptide with a constrained beta-turn on the YSNS residue has been observed to exhibit antiangiogenic activities both *in vitro* and *in vivo* (Thevenard et al. 2010). Since αvβ3 integrin are specifically expressed in the tumor vasculature, CNYYSNS can home into tumors by initially binding to these integrin. Considering this property, the short CNYYSNS peptide, corresponding to residues 185–191 of the NC1[a3(IV)] domain of type IV collagen, hereinafter called tumstatin7, may be a potent and specific anti-tumor antagonist of the αvβ3 integrin (Floquet et al. 2004).

Poor penetration into tumor tissues is a key obstacle limiting the therapeutic efficacy of many anti-cancer drugs and potential candidates (Hambley 2009; Minchinton and Tannock 2006) including tumstatin7. Herein, we report a newly developed strategy to improve the peptide-mediated delivery of tumstatin7 deep into the tumor parenchyma. The tissue-penetrating peptide we selected for this purpose is a basic 11-residue domain of the HIV-1 trans-acting activator of the transcription protein, hereinafter referred to as TAT (amino acid sequence=YGRKKRRQRRR)(Brooks et al. 2005; Murriel and Dowdy 2006; Rizzuti et al. 2015; Schwarze and Dowdy 2000; Schwarze et al. 1999; Zhang et al. 2012; Ziegler and Seelig 2004).

TAT may carry peptide drugs into tumor tissues when it is chemically conjugated to them (Koren and Torchilin 2012). For example, TAT can carry the BH3 (Bcl-2 homology 3) effectors domain from a PUMA (p53 upregulated modulator of apoptosis) plus DV3 (the binding domain of the C-X-C motif receptor 4 ligand) fusion peptide into tumor tissues by chemically conjugation to the fusion peptide, resulting in effective induction of cancer apoptosis and inhibition of cancer growth in vivo(Liu et al. 2009). TAT has been utilized as a powerful tumor-penetrating peptide in many several other studies (Benavent Acero et al. 2014; Liu et al. 2012; Liu et al. 2014).

In our strategy, TAT was conjugated to the C-terminus of tumstatin7 with an ordinary GG linker between them to generate a novel peptide we denoted as tumstatin7-TAT. We hypothesized that TAT, a domain with tissue-penetrating properties, can be utilized to deliver tumstatin7 into the tumor parenchyma and that tumstatin7-TAT can be expected to exhibit antitumor, tumor-homing, and tumor penetration properties.

In this work, we describe the functions of a peptide that combines tissue-penetrating and antitumor properties. We also evaluated the potential use of tumstatin7-TAT in tumor therapy by performing tumor treatment studies *in vitro* and *in vivo*.

2. Investigations and results

2.1. Tumstatin7-TAT exhibited better antiproliferative effects than tumstatin7 in vitro

To test whether introduction of TAT would enhance the activity of tumstatin7 *in vitro*, we performed MTT assays on treated cells. Figure 1 indicates that addition of TAT to the C-terminus of tumstatin7 generally enhanced its basal antiproliferative activity in several tumor cell lines.

Tumstatin7-TAT exhibits significantly higher antiproliferative activity than tumstatin7 (p value <0.001) in B16F10 cells; the latter exhibited antiproliferative activity only at the highest concentration applied (>200 μmol/L). Tumstatin7-TAT exhibited significant antiproliferative activities at high concentrations (≥3.125 μmol/L) in a dose-dependent manner. For instance, tumstatin7-TAT inhibited B16F10 melanoma cell proliferation by 18.0% at 12.5 μmol/L,

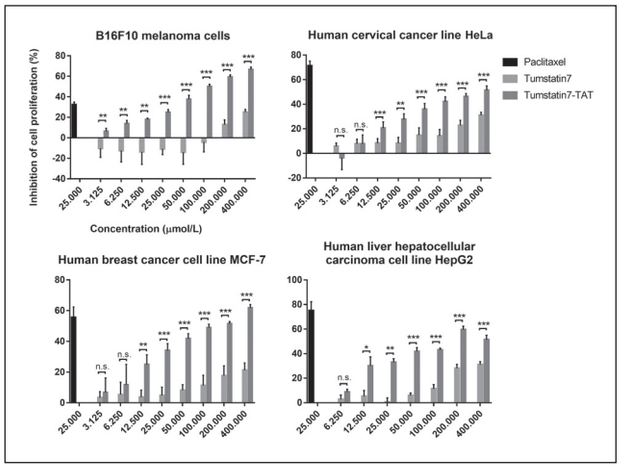

Fig. 1: Tumstatin7-TAT and tumstatin7 inhibit cancer cell proliferation. Tumstatin7-TAT or tumstatin7 was added to cell suspensions, and cells were incubated for 48 h and examined by MTT assay. Paclitaxel (25 μmol/L) was set as the positive control, and RPMI 1640 was set as the negative control. All of the data are expressed as mean±standard deviation. Statistical analyses were performed with Student's *t*-test; n.s., not significant; *p < 0.05; **p < 0.01; ***p < 0.001.

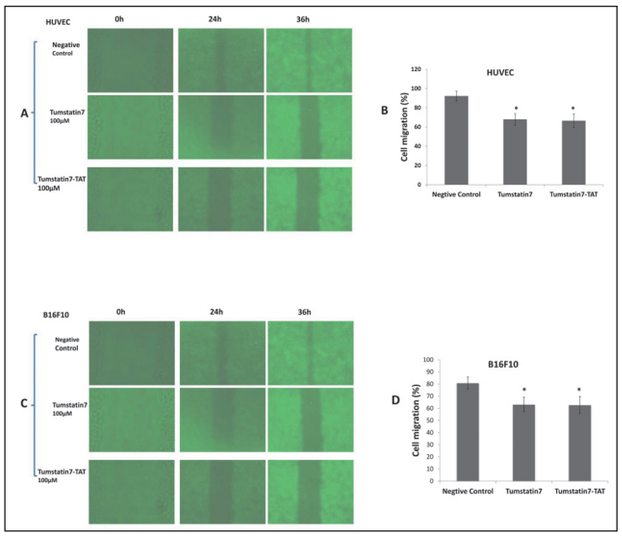

Fig. 2: Tumstatin7-TAT and tumstatin7 inhibit cell migration. HUVEC or B16F10 cells were seeded on 12-well plates. An artificial wound was made with a 100-1000 μL pipet tip (arrows) and photographs were obtained 0, 24, and 36 h later under a phase-contrast inverted microscope. The column chart represents percentage of cell migration at 36 h. Migration was calculated using Image J software. Date were analyzed using one-way ANOVA followed by post hoc Tukey HSD test using R Software Version 3.3.1. Error bars, mean±SEM; n.s., not significant; *p < 0.05; **p < 0.01; ***p < 0.001.

whereas tumstatin7 showed no antiproliferative activity at the same concentration (*p* value <0.001). These results indicated that conjugation of TAT to the C-terminus of tumstatin7 could increase its basal antiproliferative activity against the B16F10 melanoma cell line.

Compared with tumstatin7, treatment with rumstatin7-TAT induced a significantly higher inhibition of cell growth in HeLa cells. For example, at 25.0 μmol/L, tumstatin7-TTD inhibited HeLa cell proliferation by 27.7 %, whereas tumstatin7 inhibited proliferation by only 8.3 % (*p* value < 0.01).

The MCF-7 cell line was treated with tumstatin7 or tumstatin7-TAT at doses ranging from 3.125 μmol/L to 400 μmol/L. Both tumstatin7 and tumstatin7-TAT exhibited anti-proliferative activities in a dose-dependent manner, but the growth inhibition induced by the latter was significantly higher than that induced by the former at the same dose. For instance, tumstatin7-TAT at 25 μmol/L inhibited MCF-7 proliferation by 34.1 %, whereas tumstatin7 inhibited proliferation by only 4.8 % (*p* value < 0.001).

When HepG2 cells were treated with tumstatin7 or tumstatin7-TAT at doses ranging from 6.5 μmol/L to 400 μmol/L, tumstatin7-TAT also exhibited significantly higher antiproliferative activity than tumstatin7. For instance, tumstatin7-TAT inhibited HepG2 cell proliferation by 33.1 % at 50 μmol/L, whereas tumstatin7 showed no antiproliferative activity at the same concentration (*p* value <0.001). These results indicated that conjugation of TAT to the C-terminus of tumstatin7 could increase its basal antiproliferative activity against various cancer cell lines.

2.2. Tumstatin7-TATinhibited endothelial and B16F10 cell migration

The effects of tumstatin7 and tumstatin7-TAT on HUVEC and B16F10 cell migration *in vitro* were determined by a scratch-wound assay. The results of this assay are shown in Fig. 2. HUVECs migrated to the wound area and healed it by 92 % after 36 h. Treatment with tumstatin7 and tumstatin7-TAT decreased this migration by 68% and 67%, respectively. By comparison, B16F10 cells migrated to the wound and healed it by 81 % after 36 h. Treatment with tumstatin7 decreased this migration by 63 % after 36 h, while treatment with tumstatin7-TAT slowed down wound repair by 62 % at the same time point. As expected, these results showed that tumstatin7-TAT possessed the same cell-migration inhibitory activity as tumstatin7.

2.3. Tumstatin7-TAT was significantly more effective in inducing apoptosis in B16F10 cells than tumstatin7

B16F10 cells treated with tumstatin7 or tumstatin7-TAT at a concentration of 0.4 μmol/mL for 48 h showed characteristic apoptotic changes. Both tumstatin7 and tumstatin7-TAT induced apoptosis as ascertained by Annexin V-FITC/PI double staining tests (Fig. 3). The results of double staining showed that the percentage of apoptotic cells treated with tumstatin7-TAT increased to 31.95% compared with that induced by tumstatin7 (4.39%) at the same dose. Fluorescence *in situ* was then performed and observed by fluorescent inverted microscope. Result shows that tumstatin7 or tumstatin7-TAT induced decrease in cell number. Quite a lot cells turned into round cell morphology and a considerable amount of B16F10 cells were stained as green or orange-red with Annexin V-FITC or PI when treated with tumstatin7-TAT. These results indicated that tumstatin7-TAT was significantly more effective in inducing apoptosis in B16F10 cells than tumstatin7 and further confirmed that addition of TAT to the C-terminus of tumstatin7 increased its apoptotic function relative to that of tumstatin7 in B16F10 cells.

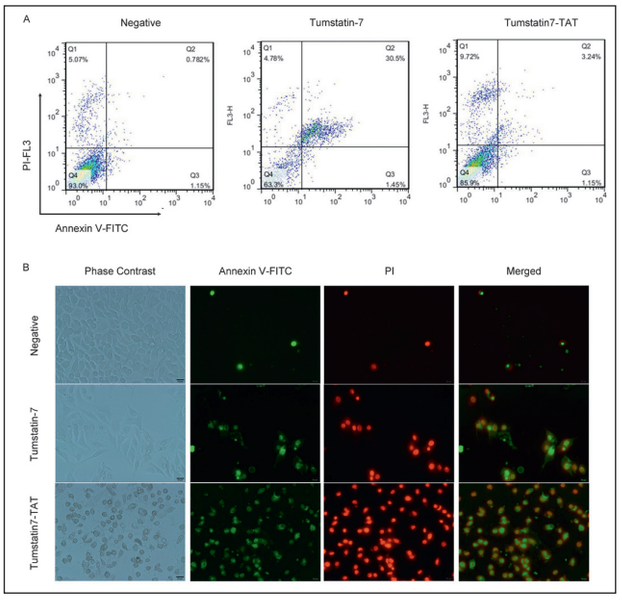

Fig. 3: Tumstatin7-TAT induces more potent effects on apoptosis than tumstatin7 in B16F10 cells. Assessment of apoptosis induced by tumstatin7-TAT or tumstatin7 at a concentration of 400 μmol/L via Annexin V-FITC/PI staining.

2.4. *Tumstatin7-TAT exhibited better effects than tumstatin7 on tumor growth inhibition in vivo*

The *in vivo* antitumor effect of tumstatin7-TAT was compared with that of tumstatin7 using a mouse tumor model with time-dependent tumor volume measurements. Subsequent injections of tumstatin7 or tumstatin7-TAT were performed as described in the Experimental section. Tumstatin7-TAT exhibited more potent tumor growth inhibitory activity than tumstatin7. Seven tumor entities of each group were lined as Fig. 4A shows. On day 8, the average tumor volume of mice treated with tumstatin7 and tumstatin7-TAT was 836±173 mm^3 ($p<0.05$) and 742±67 mm^3 ($p<0.01$), respectively, compared to the PBS group (Table, Fig. 4B). Similarly, tumor weight was also induced to varying degrees treated with tumstatin7 and tumstatin7-TAT which is 0.82±0.20 g and 0.70±0.16 g ($p<0.05$), respectively, compared to 1.08±0.35 g of the PBS group (Fig. 4C). The tumor inhibitory rate is shown in Fig. 4D. Tumstatin7-TAT showed an increased anti-tumor activity without obvious side effects, e.g. body weight loss, while paclitaxel group do have a loss of body weight ($p<0.05$) in contrast of PBS group (Fig. 5).

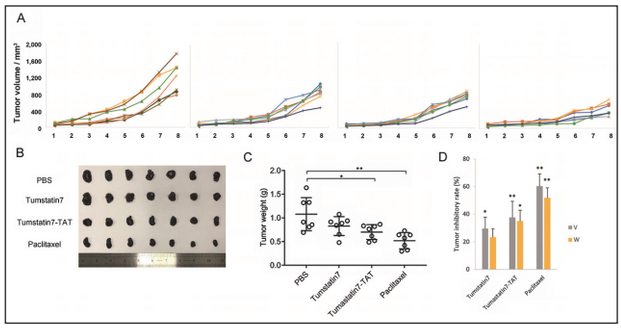

Fig. 4: Tumstatin7-TAT and tumstatin7 inhibit in vivo tumor growth. B16F10 cells were subcutaneously injected into C57Bl6 mice (5×10^6 cells/mouse). Subsequent injections of Tumstatin7-TAT or tumstatin7 (10 mg/kg) were performed on days 1, 3, 5, 7 and 9. A. Tumor volume. B. The tumor entity. C. Tumor weight. D. The tumor inhibitory rate.

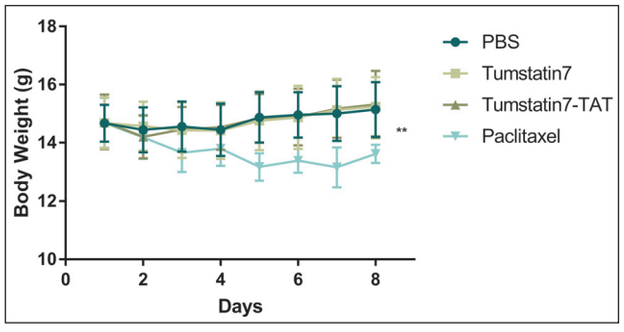

Fig. 5: Body weight of C57BL/6 mice. Body weight of C57BL/6 mice were measured every day when they were divided into difference groups. Date were analyzed using one-way ANOVA followed by post hoc Tukey HSD test using R Software Version 3.3.1. Error bars, mean ± SEM; n.s., not significant; *p < 0.05; **p < 0.01; ***p < 0.001.

Table: Tumor inhibitory rate of tumor volume and tumor weight in melanoma (n=7)

Inhibition rate (%)	Tumstatin7	Tumstatin7-TAT	Paclitaxel
Tumor volume	29.63 (P=0.0339)	37.60 (P=0.0056)	60.36 (P=0.00002)
Tumor weight	23.33 (P=0.2043)	34.99 (P=0.0265)	51.89 (P=0.0008)

The difference was analyzed compared with PBS group.

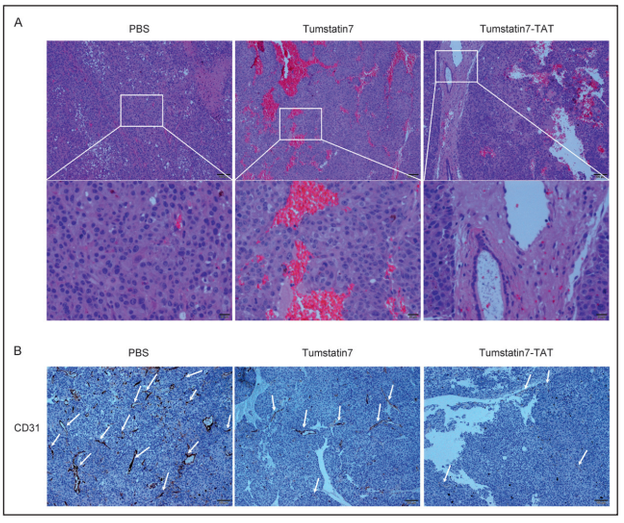

Fig. 6: Tumstatin7-TAT and tumstatin7 lead to tumor necrosis and increased expression of CD31. A. H&E staining of B16F10 tumor tissues. The nucleus was stained as blue by hematoxylin, whereas the cytoplasm was stained as pink by eosin. Scale bars, 20 μm. B. Immunohistochemistry to CD31. Arrows represent CD31 expression in tumor tissues. Scale bars, 100 μm.

Tumor entities were sliced and stained by hematoxylin and eosin. There were many cells with nuclear structure and partial necrosis area in the paraffin sections of tumor treated with PBS or tumstatin7, while in the tumstatin7-TAT group, there was a larger necrosis area with more shrinking tumor cells or nuclear -disappeared cells (Fig. 6A). Vessels supply nutrient for tumor growth. By using immunohistochemistry, the expression level of CD31 was determined to evaluate the content of vessels. As Figure 6B shows, both tumstatin7 and tumstatin7-TAT can reduce the expression of CD31 while tumstatin7-TAT showed a better activity on inhibiting the proliferation of vessels.

2.5. *Both tumstatin7-TAT and tumstatin7 showed similar cell adhesion*

To ascertain whether tumstatin7 or tumstatin7-TAT could regulate cell attachment in B16F10 cells, we performed a cell attachment

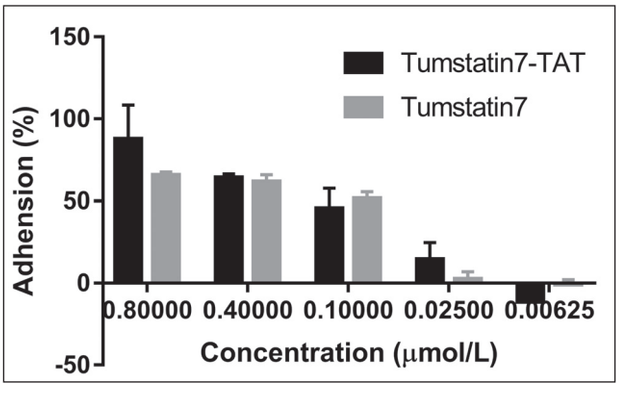

Fig. 7: Tumstatin7-TAT and tumstatin7 show similar cell adhesion properties. Cells bound to the wells were fixed and then stained with 0.5% crystal violet staining buffer. The crystal violet was extracted and the remaining adherent B16F10 cells were recorded by a microplate spectrophotometer at 595 nm. All data are expressed as mean ± standard deviation. Statistical analyses were performed with Student's *t*-test; *p < 0.05; **p < 0.01; ***p < 0.001.

assay, the results of which are shown in Fig. 7. Both compounds exhibited similar cell attachment activities in a concentration-dependent manner. For instance, the relative cell adhesion (%) of tumstatin7-TAT at 800 μmol/L was 87.56% whereas that of tumstatin7 was 65.66% at the same dose. The slight enhancement in cell adhesion

properties of tumstatin7-TAT in comparison with that of tumstatin7 was not statistically significant. In another instance, the relative cell adhesion (%) of tumstatin7-TAT at 400 µmol/L was 64.03 % whereas that of tumstatin7 was 61.54 % at the same dose ($p>0.05$). This finding indicated that conjugation of TAT to the C-terminus of tumstatin7 did not change its cell adhesion activity.

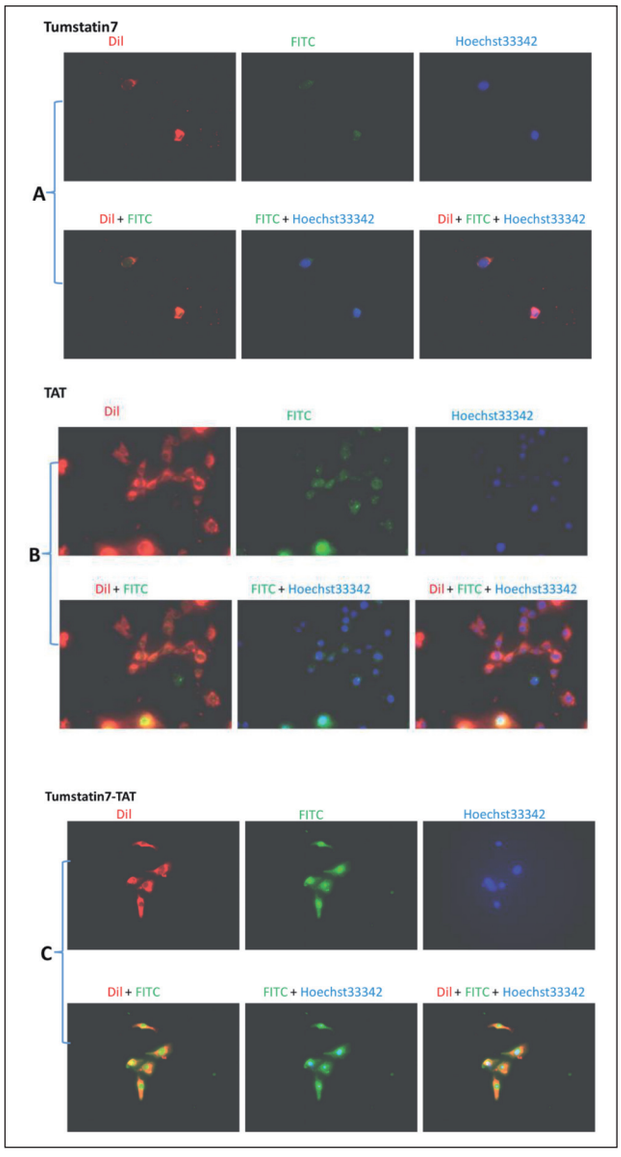

Fig. 8: Tumstatin7-TAT is capable of cell penetration. Cells were fixed with formaldehyde and labeled with FITC-labeled peptides (green), DiI (cell membrane; red), and Hoechst 33342 (blue). Nuclei were counterstained with Hoechst 33342 (blue). In the merged images, yellow areas show co-localization of the cell membrane and FITC labeled peptides while cyan areas show co-localization of the cell nuclei and FITC labeled peptides. A. Tumstatin7. B.TAT(YGRKKRRQRRR). C. Tumstatin7-TAT.

2.6. *Tumstatin7-TAT was capable of cell penetration*

Because TAT induces cell penetration, we hypothesized that tumstatin7-TAT could exert effects by cell penetration. The synthesized peptide was labeled with fluorescein isothiocyanate (FITC) to trace its distribution in cells. Tumstatin7-TAT located in the cell cytoplasm and nucleus, whereas tumstatin7 located in the cell membrane (Figs. 8 A,C). After cell staining with Hoechst 33342, the tumstatin7-TAT labeled peptide partly overlapped with nuclear area of the treated cells. These results indicate that the addition of TAT to tumstatin7 endowed it with cell-penetrating properties.

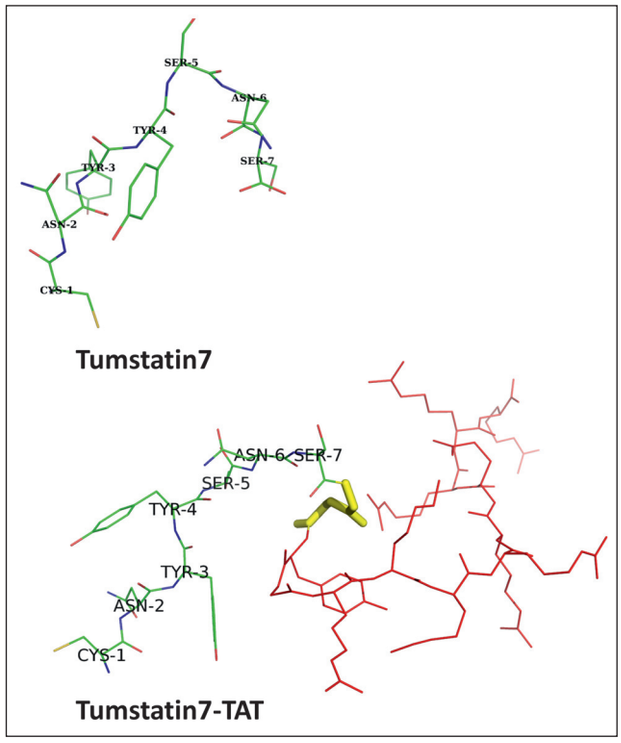

Fig. 9: Structures of the peptides determined by DSlBuilt homology model. A. Tumstatin7. B. Tumstatin7-TAT. The tumstatin7 component of tumstatin7-TAT is shown in green, the TAT component is shown in red, and the linker between them is shown in yellow.

2.7. *Three-dimensional modeling*

The 3D structures of tumstatin7 and tumstatin7-TAT were built using the computational modeling method, as shown in Fig. 9. The YSNS portions of tumstatin7-TAT and tumstatin7 in our model exhibited a specific beta-turn structure motif, which not only promotes interactions between the peptide and αvβ3 integrin but also confers other biological activities, such as antiangiogenic activity (Floquet et al. 2004). The results seem to indicate that addition of TAT to the C-terminal of tumstatin7 does not directly affect the structure of the peptide. Since structure is the basis of function, our model may explain why tumstatin7-TAT also presents antitumor activity. Moreover, based on the properties of TAT, we can assume that the enhanced antitumor activity of tumstatin7-TAT in comparison with that of tumstatin7 lies in the ability of TAT to facilitate more effective penetration of tumstatin7 into tumor cells.

3. Discussion

In this study, we compared the effectiveness of tumstatin7-TAT *in vitro* and *in vivo* with that of tumstatin7. Previous studies have indicated that tumstatin7, a N-terminal peptide composed of residues 185-191 of the NC1 domain of type IV collagen, exhibits antitumor and antiangiogenic properties *in vitro* and *in vivo* (Floquet et al. 2004).

The therapeutic efficacy and specificity of tumstatin7 is expected to increase as its capability to penetrate tumor cells is improved. Since TAT has emerged as an optimal drug carrier because of its high efficacy and pronounced cell and tissue penetrative abilities in cancer treatment (Koren et al. 2011), we proposed a strategy to improve the targeted delivery of tumstatin7 to tumor cells by adding the TAT fragment to the C-terminus of tumstatin7.

The tumstatin7-TAT fusion peptide may follow a multi-step tumor targeting mechanism. In this mechanism, tumstatin7-TAT first binds to the surface of tumor cells and then penetrates them. Several experiments support this model. First, the melanoma cell attachment assay results showed that tumstatin7-TAT shares the same attachment activity as tumstatin7. In particular, fluorescence microscopy showed

that tumstatin7-TAT was significantly internalized by B16F10 cells, whereas tumstatin7 was only located on the cell membranes. These results clearly reveal the efficacy of TAT in drug delivery.

To ascertain whether tumstatin7 or tumstatin7-TAT regulates cell motility in HUVEC and B16F10 cells, we performed a scratch-wound healing assay. Analysis of the size of the wounds (area of the scratch) after treatment indicated that tumstatin7-TAT significantly inhibited cell migration, similar to tumstatin7.

In vitro, tumstatin7-TAT inhibited the proliferation of certain tumor cells, including MCF-7, HeLa, and B16F10 cells, significantly more efficiently than tumstatin7. The former also displayed better apoptotic effects than the latter in B16F10 cells.

On the bases of these results, tumstatin7-TAT treatment induced significant inhibition of tumor growth *in vivo* in a mouse melanoma model. While both tumstatin7-TAT and tumstatin7 significantly inhibiting the expression level of CD31 and tumor growth in time-dependent tumor volume measurements *in vivo*, the former showed more significant inhibition than the latter.

Taken together, the data demonstrate that addition of TAT reinforces the antitumor activity of tumstatin7 by conferring antitumor, cell-penetrating, tumor cell-targeting properties.

In this study, we tried to connect tumstatin7 and tumor-penetrating peptide and evaluated the effectiveness of tumstatin7-TAT in tumor treatment *in vitro* and *in vivo* for the first time. This research provides an attractive strategy for maximizing the effectiveness of tumstatin7 in treating solid tumors. In future work, we aim to study the activities of this novel compound in other types of cancer cells and evaluate its pharmacokinetic and pharmacodynamic properties to improve its clinical treatment potential.

4. Experimental

4.1. Ethics

All experimental procedures using animals in this study were performed in strict compliance with recommendations from the Guide for the Care and Use of Laboratory Animal supported by the United States National Institutes of Health and approved by the Jiangsu Provincial Experimental Animal Management Committee under Contract No. 2016(SU)-0010.

4.2. Materials

B16F10 mouse melanoma, human liver hepatocellular carcinoma HepG2, Henrietta Lacks strain of cancer cells HeLa, human breast cancer MCF-7, and human umbilical vein endothelial cell (HUVEC) lines were procured from our institute. Our institute purchased these cell lines from the American Type Cell Culture (Shanghai, China). Paclitaxel (Taxol) was provided by Jiangsu Yew Pharmaceutical Co., Ltd. (Wuxi, Jiangsu Province, China). C57BL/6 mice were purchased from the Comparative Medicine Center of Yangzhou University (China). The peptides used in this work, as well as their FITC labeled versions, were synthesized by Qing Dao Biopeptek Bio-tech Co., Ltd.

4.3. Inhibition of tumor cell growth

MTT assay was used to investigate inhibitory effects of tumstatin7 and tumstatin7-TAT on the five cell lines obtained; paclitaxel was set as the positive control and five replicates were set up for each tumstatin7 and tumstatin7-TAT concentration. When cells had grown to 80% confluence, 0.25% trypsin was added to the cultures to prepare cell suspensions. The cell suspensions were adjusted to a concentration of 4×10^4 cells/mL. The cell suspensions were plated on 96-well culture plate (0.1 mL/well) and inoculated for 6–8 h at 37 °C. The cells were incubated with different concentrations of tumstatin7 or tumstatin7-TAT at 37 °C. RPMI 1640 was set as the negative control and paclitaxel (25 μmol/L) was set as the positive control. After 48 h, the medium was removed and 15 μL of MTT (5 mg/mL) was added to each well. The cells were then cultured for another 4 h. The medium removed once more, and DMSO (200 μL) was used to solubilize the formazan crystals that had formed in the wells. The microplate was placed on a plate shaker for 10 min, and the absorbance of the solution was read by a microplate reader at 570 nm.

The relative inhibition of cell proliferation (%) was calculated by using the equation $(A_N - A_T)/A_N \times 100\%$, where A_T refers to the absorbance of the treatment group and A_N refers to the absorbance of the negative control group.

4.4. Cell migration assay

HUVECs and B16F10 cells (2×10^5) were separately seeded on 12-well plates. After growing to 80–90 % confluence, the cells were starved for 12 h. For the *in vitro* scratch-wound assay, a monolayer of cells was physically wounded with a 100–1000 μl pipette tip. The cells were then washed with phosphate buffered saline (PBS) three times and incubated with or without 0.1 μmol/mL tumstatin7 or tumstatin7-TAT in 10% FBS+RPMI 1640.The area devoid of cells was photographed after 0 h, 24 h and 36 h on an inverted microscope and imaging data were acquired by Image J software.

4.5. Apoptotic assay

The apoptotic assay was performed (Lao et al. 2015; Pavlou and Kirmizis 2016) according to the kit manufacturer's instructions (Annexin V-FITC and PI Apoptosis Kit, Biouniquer, Nanjing, China). Briefly, a suspension of B16F10 cells was subjected to trypsinization, and the cells were seeded in a 6-well plate at an initial density of 2×10^5 cells/well and incubated in a humidified atmosphere of 5 % CO_2 and air at 37 °C for 6 h. Tumstatin7 or tumstatin7-TAT at a concentration of 0.4 μmol/mL was added to the wells, and the cells were incubated for 48 h; here, RPMI 1640 was used as the negative control. The cells were incubated in the presence of tumstatin7 or tumstatin7-TAT at a concentration of 0.4 μmol/mL for 48 h. Following drug treatment, the cells were washed with cold PBS followed by trypsinization. For each sample, 4×10^5 cells were counted and resuspended in a binding buffer, followed by incubation with 5 μL of AnnexinV-FITC and 5 μL of propidiumiodide for 10 min in the dark. Apoptotic cells were determined using a FACScan flow cytometer (BD Biosciences).

4.6. Tumor models

Five-week-old female C57BL/6 mice were purchased from Comparative Medicine Center of Yangzhou University (China). Suspensions of B16F10 cells (5×10^6 cells in 0.1 mL of PBS) were implanted subcutaneously on the mid-left side of C57B/6 mice. When the average tumor volume of B16F10 mouse melanoma reached 100 mm^3, the mice were divided into four groups (7 mice/group). The first group of mice was injected with 0.1 mL of PBS at a site distant from the tumor, the second group with 0.1 mL of tumstatin7, the third group with 0.1 mL of tumstatin7-TAT, and the fourth group with paclitaxel (10 mg/[kg.2d]). For the second and third groups, subcutaneous injections of tumstatin7 (10 mg/kg) or tumstatin7-TAT (10 mg/kg) were performed on day 1, day 3, day5, day 7 and day 9. Tumor sizes were measured every two days and determined according to the formula: tumor volume = $A\times B^2\times0.5$, where A is the largest dimension of the tumor and B is the smallest dimension. Therapeutic effects on tumor growth are presented as percentages of tumor suppression, calculated as $(1 - T/C) \times100\%$, where T denotes the treated tumor volume and C represents the control tumor volume.

4.7. B16F10 melanoma cell attachment assay

Cell attachment experiments were performed as previously described (Lao et al. 2013; Wang et al. 2011). A 96-well ELISA plate was first coated with various concentrations of tumstatin7-TAT or tumstatin7 at 4 °C overnight and then blocked with 2% bovine serum albumin in RPMI 1640 medium at 37 °C for 2 h. Wells were washed three times with PBS before addition of 100 μL of B16F10 melanoma cells (3×10^4/100 μL) to each well and incubation for 1 h at 37 °C. Unbound cells were removed by three washes with isotonic saline buffer. Attached cells were fixed in PBS containing 3% paraformaldehyde and 2% saccharine, stained with 0.5% crystal violet, examined by phase-contrast microscopy, photographed, and finally lysed in 10% acetic acid (100 μL per well). The OD of the solution in each well was measured at 595 nm.

4.8. Peptide labeling and microscope analysis

The peptides and their FITC-labeled versions were synthesized by Qing Dao Biopeptek Bio-tech Co., Ltd., purified by high-performance liquid chromatography, and confirmed by mass spectrometry. B16F10 cells were first incubated with the FITC-labeled peptides for 30 min and washed twice with PBS. After incubation with DiI for 20 min, the cells were incubated with Hoechst 33342 for 10 min and observed under an inverted fluorescence microscope. DiI was used to stain cell membranes and Hoechst 33342 was used to stain cell nuclei. After three washes with PBS, the B16F10 cells were examined by a microscope and photographed.

4.9. Modeling of the structures of tumstatin7-TAT and tumstatin7

The structure of tumstatin7 was modeled using the DS|Built homology model (Accelrys Inc., USA) based on a template (PDB file 1LI1) (Than et al. 2002). The structure of tumstatin7-TAT was also modeled using the same method based on two templates (PDB file 1LI1 and PDB file1TIV (Bayer et al. 1995)). The initial models were optimized by performing a set of minimization and equilibration steps followed by molecular dynamics calculations using the CHARMm force field.

Acknowledgements: This work was supported by the National Natural Science Foundation of China (Grant No. 31300643 and No. 31370505), the Fundamental Research Funds for the Central Universities (Fund No.2632018ZD04), the Priority Academic Program Development of Jiangsu Higher Education Institutions (PAPD) and Top-notch Academic Programs Project of Jiangsu Higher Education Institutions (TAPP). The funders had no role in study design, data collection and analysis, decision to publish, or preparation of the manuscript.

Conflict of interest: The authors declared no conflict of interest.

Author contributions: Conceived and designed the experiments: Xingzhen Lao and Heng Zheng. Performed the experiments and analyzed the data: Xingzhen Lao, Ran Zhang, Bin Li, Qingqing Li, Fanwen Wang.

References

Bayer P, Kraft M, Ejchart A, Westendorp M, Frank R, Rosch P (1995) Structural studies of HIV-1 Tat protein. J Mol Biol 247: 529-535.

Benavent Acero FR, Perera Negrin Y, Alonso DF, Perea SE, Gomez DE, Farina HG (2014) Mechanisms of cellular uptake, intracellular transportation, and degrada-

tion of CIGB-300, a Tat-conjugated peptide, in tumor cell lines. Mol Pharm 11: 1798-1807.
Brooks H, Lebleu B, Vives E (2005) Tat peptide-mediated cellular delivery: back to basics. Adv Drug Del Rev 57: 559-577.
Caudroy S, Cucherousset J, Lorenzato M, Zahm JM, Martinella-Catusse C, Polette M, Birembaut P (2004) Implication of tumstatin in tumor progression of human bronchopulmonary carcinomas. Human Pathol 35: 1218-1222.
Fawzi A, Robinet A, Monboisse JC, Ziaie Z, Kefalides NA, Bellon G (2000) A peptide of the alpha 3(IV) chain of type IV collagen modulates stimulated neutrophil function via activation of cAMP-dependent protein kinase and Ser/Thr protein phosphatase. Cell Signal 12: 327-335.
Floquet N, Pasco S, Ramont L, Derreumaux P, Laronze JY, Nuzillard JM, Maquart FX, Alix AJ, Monboisse JC (2004) The antitumor properties of the alpha3(IV)-(185-203) peptide from the NC1 domain of type IV collagen (tumstatin) are conformation-dependent. J Biol Chem 279: 2091-2100.
Hambley TW (2009) Is anticancer drug development heading in the right direction? Cancer Res 69: 1259-1261.
Han J, Ohno N, Pasco S, Monboisse JC, Borel JP, Kefalides NA (1997) A cell binding domain from the alpha3 chain of type IV collagen inhibits proliferation of melanoma cells. J Biol Chem 272: 20395-20401.
Koren E, Apte A, Sawant RR, Grunwald J, Torchilin VP (2011) Cell-penetrating TAT peptide in drug delivery systems: proteolytic stability requirements. Drug Del 18: 377-384.
Koren E, Torchilin VP (2012) Cell-penetrating peptides: breaking through to the other side. Trends Mol Med 18: 385-393.
Lao X, Liu M, Chen J, Zheng H (2013) A tumor-penetrating peptide modification enhances the antitumor activity of thymosin alpha 1. PloS one 8: e72242.
Lao XZ, Li B, Liu M, Shen C, Yu TT, Gao XD, Zheng H (2015) A modified thymosin alpha 1 inhibits the growth of breast cancer both in vitro and in vivo: suppressment of cell proliferation, inducible cell apoptosis and enhancement of targeted anticancer effects. Apoptosis 20: 1307-1320.
Liu RH, Xi L, Luo DF, Ma XY, Yang WH, Xi YD, Wang HY, Qian M, Fan LS, Xia X, Li KZ, Wang DW, Zhou JF, Meng L, Wang SX, Ma D (2012) Enhanced targeted anticancer effects and inhibition of tumor metastasis by the TMTP1 compound peptide TMTP1-TAT-NBD. J Control Release 161: 893-902.
Liu YJ, Li YF, Wang HJ, Yu J, Lin HW, Xu DK, Wang Y, Liang AL, Liang X, Zhang XY, Fu M, Qian HL and Lin C (2009) BH3-based fusion artificial peptide induces apoptosis and targets human colon cancer. Mol Ther 17:1509-1516.
Liu Z, Xiong M, Gong JB, Zhang Y, Bai N, Luo YP, Li LY, Wei YQ, Liu YH, Tan XY, Xiang R (2014) Legumain protease-activated TAT-liposome cargo for targeting tumours and their microenvironment. Nat Commun 5: 4280.
Maeshima Y, Colorado PC, Kalluri R (2000a) Two RGD-independent alpha vbeta 3 integrin binding sites on tumstatin regulate distinct anti-tumor properties. J Biol Chem 275: 23745-23750.
Maeshima Y, Colorado PC, Torre A, Holthaus KA, Grunkemeyer JA, Ericksen MB, Hopfer H, Xiao Y, Stillman IE, Kalluri R (2000b) Distinct antitumor properties of a type IV collagen domain derived from basement membrane. J Biol Chem 275: 21340-21348.
Maeshima Y, Sudhakar A, Lively JC, Ueki K, Kharbanda S, Kahn CR, Sonenberg N, Hynes RO, Kalluri R (2002) Tumstatin, an endothelial cell-specific inhibitor of protein synthesis. Science 295: 140-143.
Minchinton AI, Tannock IF (2006) Drug penetration in solid tumours. Nat Rev Cancer 6: 583-592.
Murriel CL, Dowdy SF (2006) Influence of protein transduction domains on intracellular delivery of macromolecules. Expert Opin Drug Del 3: 739-746.
Pasco S, Han J, Gillery P, Bellon G, Maquart FX, Borel JP, Kefalides NA, Monboisse JC (2000a) A specific sequence of the noncollagenous domain of the alpha3(IV) chain of type IV collagen inhibits expression and activation of matrix metalloproteinases by tumor cells. Cancer Res 60: 467-473.
Pasco S, Monboisse JC, Kieffer N (2000b) The alpha 3(IV)185-206 peptide from noncollagenous domain 1 of type IV collagen interacts with a novel binding site on the beta 3 subunit of integrin alpha Vbeta 3 and stimulates focal adhesion kinase and phosphatidylinositol 3-kinase phosphorylation. J Biol Chem 275: 32999-33007.
Pasco S, Ramont L, Venteo L, Pluot M, Maquart FX, Monboisse JC (2004) In vivo overexpression of tumstatin domains by tumor cells inhibits their invasive properties in a mouse melanoma model. Exp Cell Res 301: 251-265.
Pavlou D, Kirmizis A (2016) Depletion of histone N-terminal-acetyltransferase Naa40 induces p53-independent apoptosis in colorectal cancer cells via the mitochondrial pathway. Apoptosis 21: 298-311.
Rizzuti M, Nizzardo M, Zanetta C, Ramirez A, Corti S (2015) Therapeutic applications of the cell-penetrating HIV-1 Tat peptide. Drug Discov Today 20: 76-85.
Schwarze SR, Dowdy SF (2000) In vivo protein transduction: intracellular delivery of biologically active proteins, compounds and DNA. Trends Pharmacol Sci 21: 45-48.
Schwarze SR, Ho A, Vocero-Akbani A, Dowdy SF (1999) In vivo protein transduction: Delivery of a biologically active protein into the mouse. Science 285: 1569-1572.
Shahan TA, Ziaie Z, Pasco S, Fawzi A, Bellon G, Monboisse JC, Kefalides NA (1999) Identification of CD47/integrin-associated protein and alpha(v)beta3 as two receptors for the alpha3(IV) chain of type IV collagen on tumor cells. Cancer Res 59: 4584-4590.
Sudhakar A, Sugimoto H, Yang C, Lively J, Zeisberg M, Kalluri R (2003) Human tumstatin and human endostatin exhibit distinct antiangiogenic activities mediated by alpha v beta 3 and alpha 5 beta 1 integrins. Proc Natl Acad Sci USA 100: 4766-4771.
Than ME, Henrich S, Huber R, Ries A, Mann K, Kuhn K, Timpl R, Bourenkov GP, Bartunik HD, Bode W (2002) The 1.9-angstrom crystal structure of the noncollagenous (NC1) domain of human placenta collagen IV shows stabilization via a novel type of covalent Met-Lys cross-link. Proc Natl Acad Sci USA 99: 6607-6612.
Thevenard J, Ramont L, Devy J, Brassart B, Dupont-Deshorgue A, Floquet N, Schneider L, Ouchani F, Terryn C, Maquart FX, Monboisse JC, Brassart-Pasco S (2010) The YSNSG cyclopeptide derived from tumstatin inhibits tumor angiogenesis by down-regulating endothelial cell migration. Int J Cancer 126: 1055-1066.
Wang P, Ballestrem C, Streuli CH (2011) The C terminus of talin links integrins to cell cycle progression. J Cell Biol 195: 499-513.
Zhang XK, Zhang X and Wang FS (2012) Intracellular transduction and potential of Tat PTD and its analogs: from basic drug delivery mechanism to application. Expert Opin Drug Delivery 9: 457-472.
Ziegler A, Seelig J (2004) Interaction of the protein transduction domain of HIV-1 TAT with heparan sulfate: Binding mechanism and thermodynamic parameters. Biophys J 86: 254-263.